Ultrasonic Attenuation in Steel and Cast Iron

Ultrasonic Attenuation in Steel and Cast Iron*

Kazuo KAMIGAKI

The Research Institute for Iron, Steel and Other Metals

(Received December 13, 1956)

Synopsis

Ultrasonic attenuation in steel and cast iron with various kinds of texture were measured in the frequency range from 0.5 to 25 megacycles per second making use of pulsed longitudinal ultrasonic waves. For this purpose, several processes of heat treatments were applied successively to the same specimens and at every stage of such treatments the attenuation measurements were carried out. The chromium-molybdenum steel and carbon steel specimens were normalized, hardened by quenching, and tempered to make the structure of troostite and sorbite, and the differences among attenuations at each stage were determined. For determining the effect of austenite grain size on the ultrasonic attenuation, the measurements were made for the carbon steel specimens heat-treated above transformation point. The white cast iron was prepared, then tempered successively till the spheroid graphite structures were reached, and the attenuations were studied at every stage of tempering. The attenuation measurements were also made both for flake graphite cast iron with various sizes of flake graphite distributing in wide range and for spheroid graphite cast iron, and the effects of the shape and size of crystallized graphite on the attenuation were studied.

The results of measurements are summarized as follows:

(1) In the case of steel ultrasonic attenuation varies remarkably with the change of the texture. In the specimens with pearlite structure, a large attenuation value was observed and the value rose steeply with frequency, so that the sound wave hardly penetrated through this medium at frequencies higher than about 10 Mc/sec. The predominant factor causing such a high attenuation is the grain size of austenite phase. In quenched specimens of martensite structure the ultrasonic attenuation was fairly low at high frequencies as 20 Mc/sec. In tempered specimens of troostite or sorbite structure, the lower attenuation values were observed. And these low attenuations are considered to be caused by the elastically anisotropic character of each grain.

(2) In cast iron the ultrasonic attenuation shows complicated dependence upon the texture. The form and size of crystallized graphite in cast iron have remarkable effect on the attenuation. White cast iron without crystallized graphite has low attenuation value. In flake graphite cast iron, very high attenuation was observed and the value increased steeply with frequency. These characters are determined directly by the size of flake graphite. The cast iron of intermediate structure, including spheroid graphite cast iron, has medium value.

(3) The most predominant factor determining the magnitude of ultrasonic attenuation is the Rayleigh scattering of ultrasound by grains. The rate of energy loss by scattering depends upon the size and elastically anisotropic character of the crystal grains.

---

* The 867th report of the Research Institute for Iron, Steel and Other Metals. This work was carried out in the laboratory of professor Tokutaro Hirone. The work was partially supported by Grant-in-Aid for Developmental Scientific Research (1952), and for Fundamental Scientific Research (Individual Research (1954) and Institutional Research (1955)) of the Ministry of Education.

I. Introduction

It has become possible since barely ten years ago to measure the ultrasonic velocity and attenuation coefficient in solid materials[1][2] with high accuracy in the megacycle frequency range by the technics of pulsed ultrasonic waves. For the metals with comparatively simple textures, such as aluminum and magnesium, e. g., considerably detailed results of ultrasonic measurements have been reported by several authors including the author of the present paper.[3][4][5] In polycrystalline specimens of these metals, the features of ultrasonic attenuation showed a remarkable dependence upon the frequency of sound waves together with the size of the crystal grains. When the wave-length is larger than the grain diameter, the energy of ultrasonic waves is scattered by each crystal grains, and in such a case the attenuation increases steeply with the frequency.[3] However, if the wave-length becomes smaller than the grain size, then the energy of the ultrasonic wave is dissipated in the course of travelling due to the reflection and the refraction at the grain boundaries, and in consequence the attenuation increases approximately in proportion with the frequency.[4] When the wave-length becomes comparable with the grain size, the scatter in phase of ultrasonic waves occurs and leads to an attenuation from polycrystalline scattering proportional to the grain size divided by the square of the wave-length.[6] These expectations from the theoretical point of view and the results of measurement were in close coincidence, and the attenuation values were affected by the magnitudes of elastic anisotropy of each crystal grain.

In the case of steel, however, there are few results available on the ultrasonic measurements in megacycle frequency range. The published results concern with the velocity and attenuation coefficient. In rolled plate of steel, the anisotropic transmission of ultrasonic waves were observed and the velocity of sound waves is different in the directions parallel and vertical to that of rolling.[7] The ultrasonic attenuation measurements have also been carried out for steel by several authors but the results have some imperfections for the precise analysis of the phenomena. It was found that the features of ultrasonic attenuation varies widely with frequency and with texture of steel specimen. In steel of normalized structure, the size of the pearlite grains is related closely with the ultrasonic attenuation. de Kerversau and others[8] have measured in pearlite specimens of various structures but the ultrasonic frequency is limited only at 5 Mc/sec. Roderick and Truell[9] have measured the ultrasonic attenuation in wide range of frequency, but

(1) H. B. Huntington, Phys. Rev., **72** (1947), 321.
(2) W. P. Mason and H. J. McSkimin, J. Acoust. Soc. America, **19** (1947), 464.
(3) W. P. Mason and H. J. McSkimin, J. Appl. Phys., **19** (1948), 940.
(4) W. Roth, J. Appl. Phys., **19** (1948), 901.
(5) T. Hirone and K. Kamigaki, Sci. Rep. RITU, **A7** (1955), 455.
(6) H. B. Huntington, J. Acoust. Soc. America, **22** (1950), 362.
(7) F. Firestone and J. Frederick, J. Acoust. Soc. America, **18** (1947), 200.
(8) E. de Kerversau, J. Bleton and P. Bastien, Rev. Metall., **46**(1949), 277 ; **47** (1950), 421.
(9) R. Roderick and R. Truell, J. Appl. Phys., **23** (1952), 267.

their measurement was confined to a few kinds of special steel specimen and systematic analysis of the origin of ultrasonic attenuation was hardly made. Generally ultrasonic attenuation in steel increases steeply with frequency and this character has been confirmed by the other authors[10][11][12] on the specimens of commercial steel, but the precise analyses were not made.

On the other hand, some technical results on ultrasonic propagation in steel have been reported in U.S.A. and Germany* concerning with the practical procedures of ultrasonic flaw inspection. But these data have dealt with the specially confined cases and unified conclusions on the nature of ultrasonic propagation cannot be obtained. (*L. Bergman, Der Ultraschall (6 Aufl.))

Now in cast iron, only few available results of ultrasonic measurement have been reported. Recently, however, the technics of ultrasonic flaw inspection have been developed for cast iron and some technical deta of the ultrasonic attenuation have been reported. But these are quite insufficient for the full description of ultrasonic propagation in this material, and as the structure of cast iron is so complicated that any unified conclusions on the acoustic properties of cast iron have not been given and many problems are left unsolved. It is generally accepted in cast iron that the ultrasonic attenuation is larger than that in steel. Hitherto ultrasonic waves of long wave-length in the range of about 0.5 – 2 Mc/sec have been used in flaw inspections of cast iron, since the attenuation of low frequency waves in cast iron is relatively small. But the testing with low frequency waves will result in lower accuracy in detecting the fine imperfections. We must consider these two conditions affecting strongly the accuracy of results in practices of flaw detection.

Thus the knowledge of the nature of ultrasonic attenuation in steel and cast iron, together with the influence of fine texture on the ultrasonic attenuation, will make more precise the technics of flaw inspection. In practice, the difference in ultrasonic attenuation between spheroid and flake graphite cast iron or between hardened and unhardened steel has been applied for the quality control of such materials. Combining the technical data with fundamental considerations, the precise analysis of the attenuation character or extended applications of the results can be expected.

The difficulties in these previous studies are due to the fact that steel and cast iron have complicated structure and the structure is altered widely by the conditions of casting and heat-treatment. It will be required to prepare so many specimens to determine all the effects of fine structure change. But, if we can prepare the series of specimen different in only single predominant character gradually, the measurements on the effects of preferential factors will be able to be carried out. Previously the present author measured the ultrasonic attenuation on aluminum with various grian sizes but other conditions are left almost in-

(10) S. Tanaka and T. Anzai, Sci. Rep. RITU, **A4** (1952), 643.
(11) A. Michalski, Stahl u. Eisen, **74** (1954), 26.
(12) K. Kato, Mem. Inst. Sci. Indust. Res., **9** (1954), 59.

variant. The similar process of preparation will lead to success of the analysis of this problem.

In this study, it was desired to obtain the general relations between the ultrasonic attenuation and the structure of steel and cast iron. The steel and cast iron specimens with various structures were prepared, and to obtain the specimens of definite structure, same pieces were heat-treated successively and uncontrollable factors influencing the ultrasonic attenuation were excluded. The measurement of ultrasonic attenuation coefficients was carried out at every successive stage of treatment on these specimens in the frequency range from 0.5 to 25 Mc/sec. The detailed description of present method of attenuation measurement and the results of observation are given in the following paragraphs.

II. Method of measurement

The apparatus used in this measurement consisted of NMM-169-C type ultrasonic flaw detector* with slight modifications and amplifier, the block diagram of which is shown in Fig. 1. The carrier frequencies are 0.5, 1, 2, 3, 5, 6, 9, 12, 15, 21 and

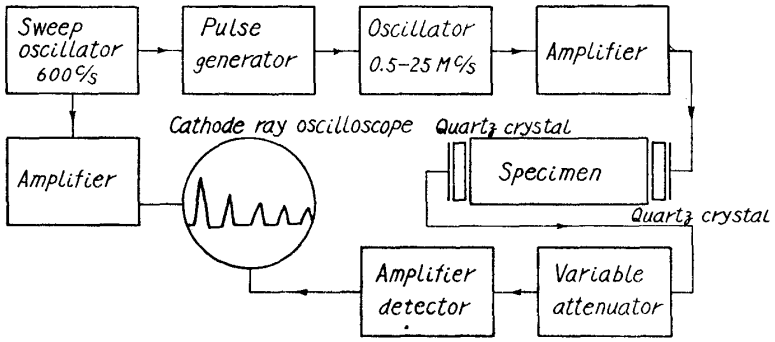

Fig. 1. The brock diagram of the apparatus.

25 Mc/s. The sine wave out-put of 600 c/s of sweep oscillator is amplifyed and differentiated into impulses of about 5 microseconds in duration and the carrier frequency oscillator is modulated by this signal. The wave form of out put signal has an approximately sinus formed envelope with a steep front. Such pulsed electric signals are fed to the x-cut quartz plate transducer, which is affixed on one of the end surfaces of the specimen by means of a thin film of oil. The ultrasonic waves thus emitted travel through the specimen and reach the receiver quartz plate affixed on the other end. The received signal is transmitted through a calibrated variable attenuator (0 to 100 decibels) into a wide band amplifier with band width of 0.5 to 2 Mc/s. Then the signal is amplified, detected and fed to the virtical axis of a cathode-ray oscilloscope and the pattern is swept by the out put of sweep oscillator. The pulsed signals are received after successive reflections at the two end surfaces and the patterns appear on the screen of cathode-ray oscilloscope as shown in the figure. The height of such pulse patterns corresponds

* Made by Japan Radio Co. Ltd.

to the amplitude of the received ultrasonic waves, and diminishes with the increasing path length. When the variable attenuator is so adjusted that each pulse appearing successively on the oscilloscope coincides with a fixed mark at the center of screen, the difference between the readings of attenuator with two successive pulses is the attenuation coefficient of ultrasonic waves during one round trip in the specimen in the unit of decibel.

The ultrasonic waves lose their energy in travelling through the medium and the lost energy is determined by the path length of the waves. The amplitude $A(x)$ of the ultrasonic waves is expressed after travelling through the distance of x cm as

$$A(x) = A(0)\exp(-\alpha x), \tag{1}$$

where α is an attenuation coefficient, and $A(0)$ is the initial amplitude. Taking logarithms of both sides, we obtain

$$-\alpha x = \log \frac{A(x)}{A(0)}. \tag{2}$$

In this measurement, a quantity proportional to the right side of the formula (2) is obtained as the reading of the variable attenuator. Thus, when the readings vary in proportion linearly to the distance travelled by the ultrasonic waves, it will be concluded that the attenuation takes a form expressed by formula (1) in the medium, and the attenuation coefficient per unit distance α can be calculated.

Now the attenuation value thus obtained contains some errors due to several causes, such as the loss of energy due to the reflection at the end-surfaces, hence some correction must be given by the method described in the previous report.[5] To correct the reflection loss, it is convenient to use two specimens of same quality but of different lengths. But as the heat-treatment of the steel specimens used for the measurement includes the procedure of quenching into water, it is impossible to make two pieces of exactly the same quality. Therefore, we had to correct the values of attenuation for reflection loss with a same specimen cutting into two pieces. At the end of the course of the measurement, we cut the specimen to encount the uniformity of the hardening, and to determine the loss due to reflection. This value of reflection loss is applied for all the measured values, and the value is about 1.2 decibles per reflection for steel. For castiron specimens, the same method cannot be used in all cases, for example, flake graphite castiron showing a very larger attenuation, but in rough estimate the loss has considerably small values between 1 and 1.5 db.

III. Specimens and heat treatments

For determining the ultrasonic attenuation coefficient, some considerations must be made for the method of the preparation of specimen. As the attenuation is very sensitive for the difference in fine structures of the specimen such as the size of grain, crystallites, precipitates and impurities, it is profitable to use the specimen of same quality. To define the quality same specimen was used for

a series of measurements and the various stuctures were prepared by successive heat-treatment, but it is impossible to alter the form of graphite crystallite in cast iron by heat-treatment, and different specimens were made from same melt. These specimens were cut into cylindrical form of precision, and mounted for the apparatus.

1. Steel

In the first place, ultrasonic attenuation coefficient in steel was measured. To prepare the specimens, steel cylinders were heat-treated in various ways of hardening and tempering, and the attenuations were measured at each stages of the working. Since the specimens used in the measurement were required to be hardened uniformly the chromium-molybdenum steel was selected and the carbon-steel was used as reference specimen. The chromium-molybdenum steel con-

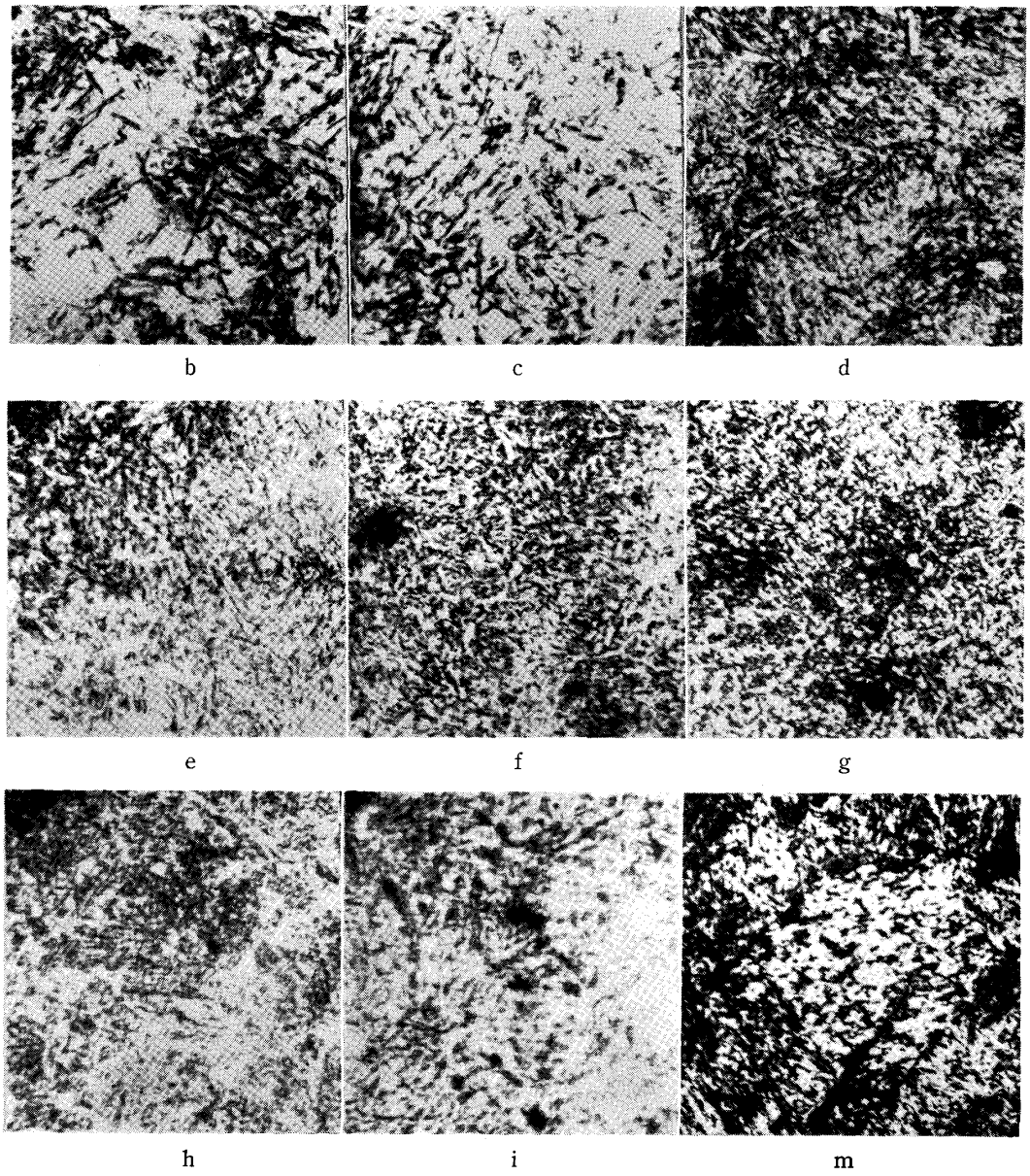

Photo. 1a. Structures of Cr–Mo steel. (×500)

Table 1. Heat treatments applied to steel specimens.

Specimen	b	c	d	e	f	g	h	i	j	k	l	m
Temperature (°C)	1000	100	200	300	400	500	600	680	800	850	1000	1000
Annealing time (hour)	1	1	1	1	1	1	1	5	1	1	1	1
Heat-treatment	Water quenched	Air cooled	,,	,,	,,	,,	,,	,,	,,	,,	,,	Water quenched

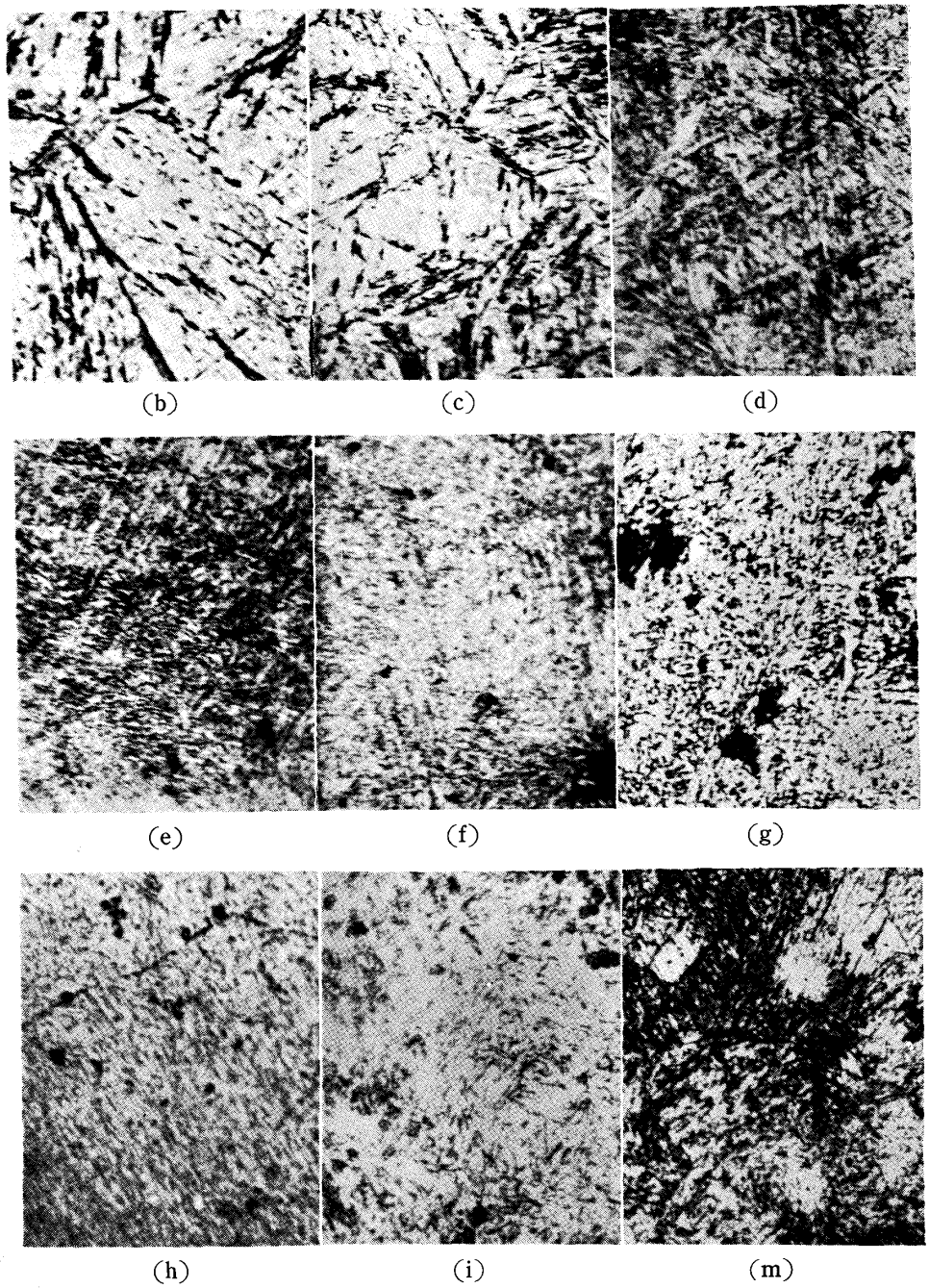

Photo. 1b. Structures of C– steel (×500)

tained C: 0.45%, Cr: 0.81%, Mo: 0.28%, Ni: 0.21% and Mn: 0.80%, and carbon steel contained 0.75% of carbon. These specimens were forged and then finished into cylinders of about 14 cm in length and about 6 cm in diameter. The two end-surfaces of the cylinder were cut parallel within the order of error of 10^{-4} in length. The corrections of the deformation after quenching and successive tempering were made by grinder finishing of the end-surfaces. The process of heat-treatment of the specimens is as shown in Table 1, and all the treatments were done in vacuum furnace. The term "air cool" in the table indicates that the specimens were cooled within the vacuum container, which was removed from the furnace without breaking the vacuum.

To confirm the uniformity of hardening, the specimen m were cut into two halves after quenching from about 1,000°C into the water. Fig. 2 shows the value of Vickers

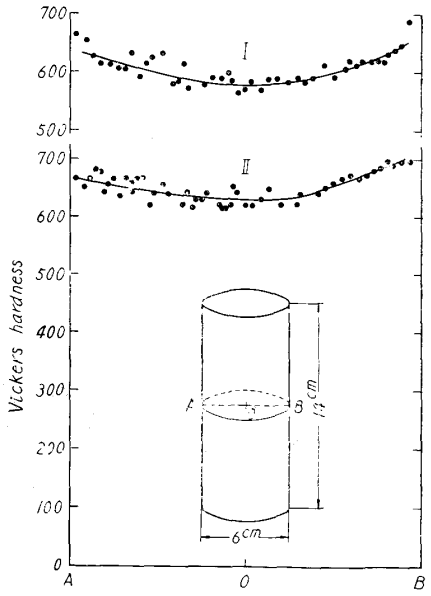

Fig. 2. Hardness along the diameter AOB of specimens.
I. Carbon steel, II. Cr-Mo steel quenched from 1000°C.

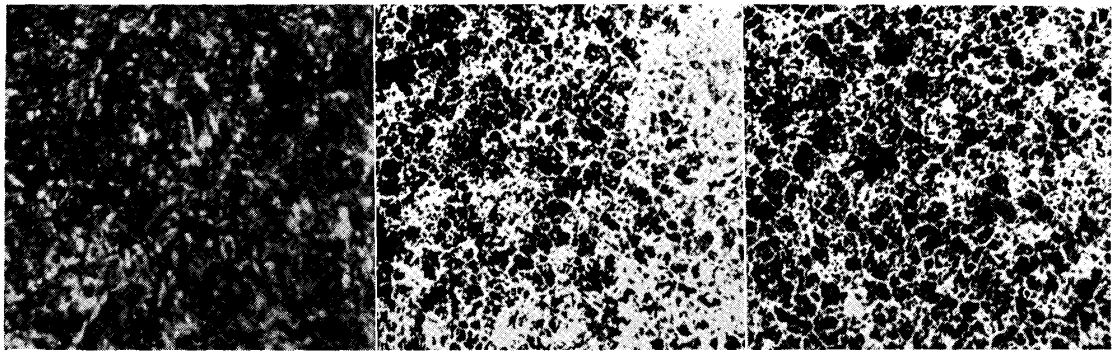

j ×500 j ×500 k ×100

Photo. 2a. Structures of Cr-Mo steel.

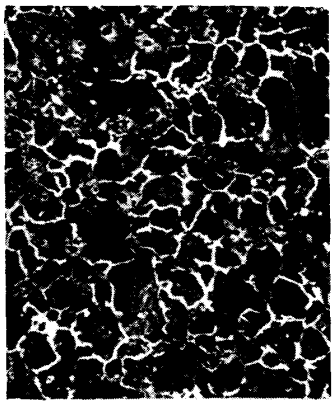

l
×100

Photo. 2b. Structures of C-steel.

hardness measured on the cut surface along the direction of diameter. Considering from the distribution of hardness value, it was concluded that the uniform hardening was brought about. The microscopic textures of the end-surfaces of the specimens were observed at each stage of heat-treatment, the results being illustrated in Photo. 1a and b. From the photographs we can easily see that martensite structures were produced by quenching, and with the progress of successive heat-treatment the structures changed gradually into troostite and then into sorbite. In the specimen annealed for 5 hours at a temperature directly below the transformation point, the sorbite structure became extremely fine. When the specimen was cooled at a rather high speed from a temperature above the

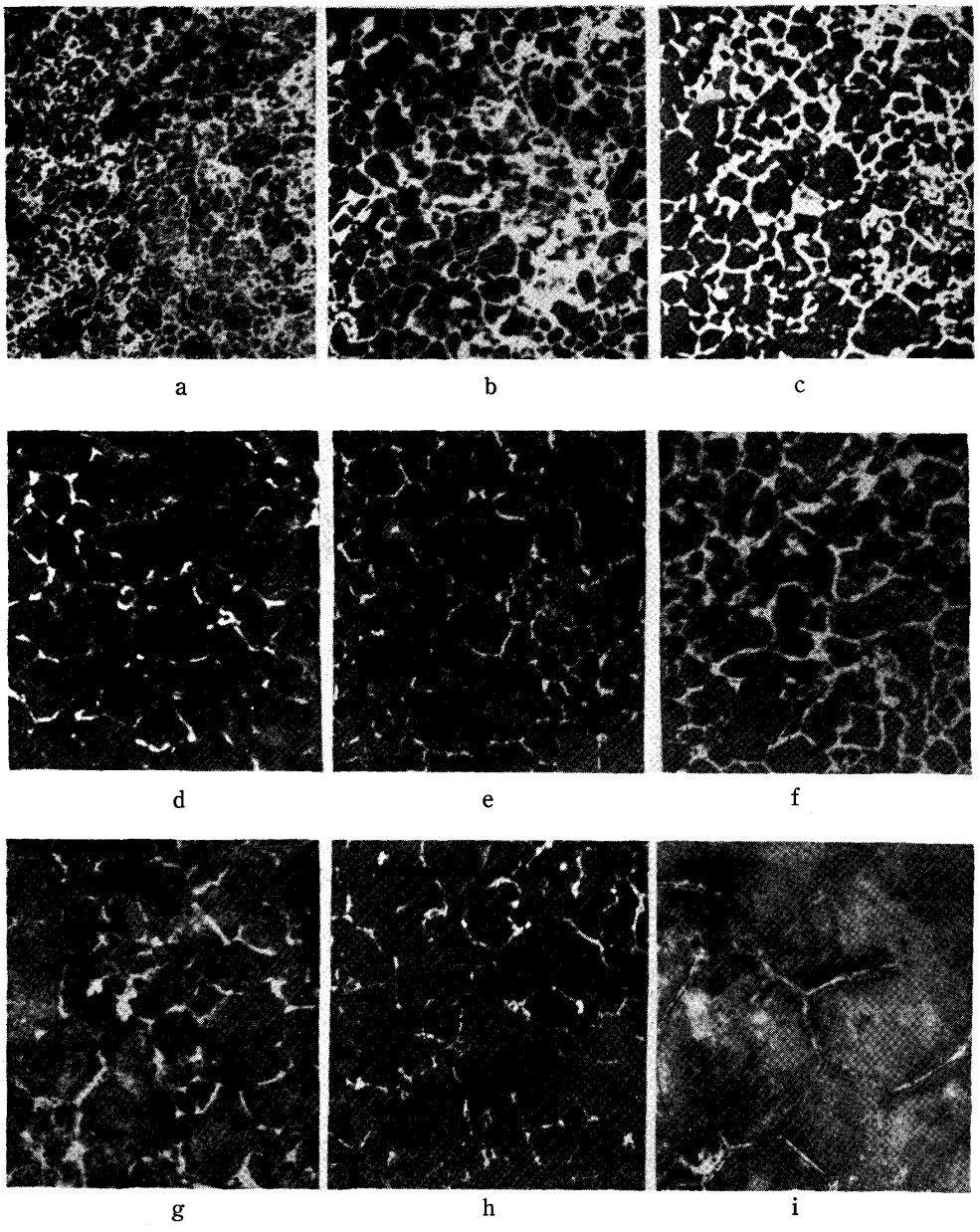

Photo. 3. Structures of normalized 0.75% carbon-steel specimen for various stages of annealing. (×100)

transformation point, a laminated pearlite structure was obtained. The pearlite structure was fine-grained and the austenite grains were classified into grain size number 7—9, as illustrated in Photo. 2a and b.

According to various reports previously published, it was found that in metals of single phase the sizes of the crystal grains have a close relation with the ultrasonic attenuation, but same effect of elementary grains has not been reported on alloys in which more than two phases coexist, such as steel. When steel is cooled down slowly from a temperature above the transformation point the pearlite structure is formed, and ferrite or cementite precipitates at the boundaries of the original austenite grains. Because the size of the austenite grains are changed with the temperature and the duration of tempering, the specimens of any grain size are prepared. In this measurement, for studying the effects of austenite grain size on the ultrasonic attenuation in steel, the carbon steel specimens were heat-treated following a program as shown in Table 2. The size of the austenite

Table 2. Heat-treatments of carbon steel specimens.

Heat treatment	a	b	c	d	e	f	g	h	i
Temperature (C)	850	950	950	1000	1050	1080	1100	1200	1300
Annealing time (hour)	1	1	5.5	1	1	5 (min.)	1	1	1
Grain size number	7–8	6–7	6–7	6–7	5–7	5–6	4–6	4–5	3–4

grains gradually increased with heat-treatment, as illustrated in the lowest row of the table, and the structure is shown in Photo. 3. For carrying out the heat-treatment at temperature higher than 1,000°C, an electric vacuum furnace with carbon-silicate heater element was used. Detailed arrangement of the furnace are shown in Fig. 3. A temperature higher than 1,200°C was obtained and it took about 1.5 hours to heat the specimen from room temperature up to this level. Lowering of temperature was made at any controlled speed by changing the electric current density. The tmperature controll was easily made, since above 600°C the electric resistance of the heater becomes metallic.

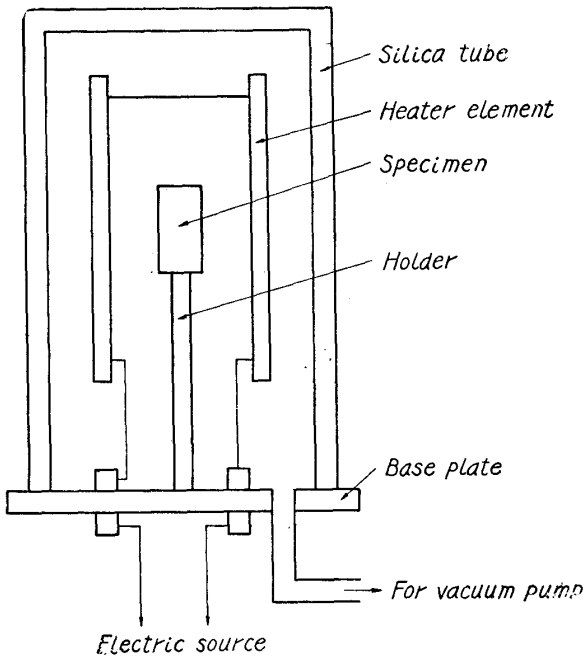

Fig. 3. Vacuum furnace for annealing below 1,300°C.

2. White cast iron

The ultrasonic attenuation in cast iron has very complicated feature and sometimes it becomes unable to analyse the results of measurement. To obtain the definite informations on the change in the attenuation values, we first proceeded to investigate the ultrasonic attenuation in specimens of white cast iron. Next, the specimens were tempered successively so as to precipitate the graphite particles from the eutectic cementite structures and measured the attenuation values on each structure. The white cast iron specimens containing 2.2 per cent of carbon and 1.4 per cent of silicon were made by electrolytic iron, pure carbon and pure silicon and were cast in steel molds of 45 mm in diameter. Then, from the ingots of either 200 mm or 120 mm in length, cylindrical specimens of 40—45 mm in diameter and 65—75 mm in length were cut out. Their end-surfaces were cut parallel, finished to flat planes and microstructure was observed at the carefully finished surfaces. The specimens were heat treated in vacuum furnace following the next program. The specimens were heated from room temperature to about 900°C in about 30 minutes, kept at the temperature for a certain duration, then cooled at 700°C in about 30 minutes, and the furnace was removed, then the specimens were cooled slowly within the vacuum container. It took about 10 minutes to cool it to 400°C and then about 20 minutes to come down to 200°C. The durations for which the specimens are kept at 900 and 700°C are as shown in Table 3.

Table 3. Heat-treatments of white cast iron specimens.

Specimen	a	b	c	d	e	f	g	h	i	j	k
Annealed at 900°C for	0 hour	+5	+5	+5	+5	+5	+1	15 min	+20	+15	+60
Annealed at 700°C for	0 hour	0	0	0	+5	+5	+75	0	0	0	0
Vickers hardness	397	225	179	145	153	152	103	279	266	238	188

The processes a—g and h—k were applied successively to the same specimens, respectively, and the ultrasonic attenuation measurements were carried out at the end of each process.

The micro-structure of the specimens was changed by the heat-treatment as shown in Photo. 4. a is white cast iron of high hardness, and in b, the structure of eutectic cementite disappeares almost completely and graphite precipitates into fine spots randomly distributed. Among the pearlite matrix small ferrite rings are found around the graphite spots. Then, in the next stage c and d, the ferrite grain grows gradually, in e and f, the graphitization is almost finished at 900°C, ferrite being in predominance, with a little domains of pearlite, and in f the low temperature graphitization is also somewhat advanced and the matrix exhausted. When f is kept at 700°C for a long time, pearlite region disappears completely, as shown in g. Its structure is composed of spheroidal graphite and ferrite grains of about 0.01 mm in diameter. For studying the effect of gradual

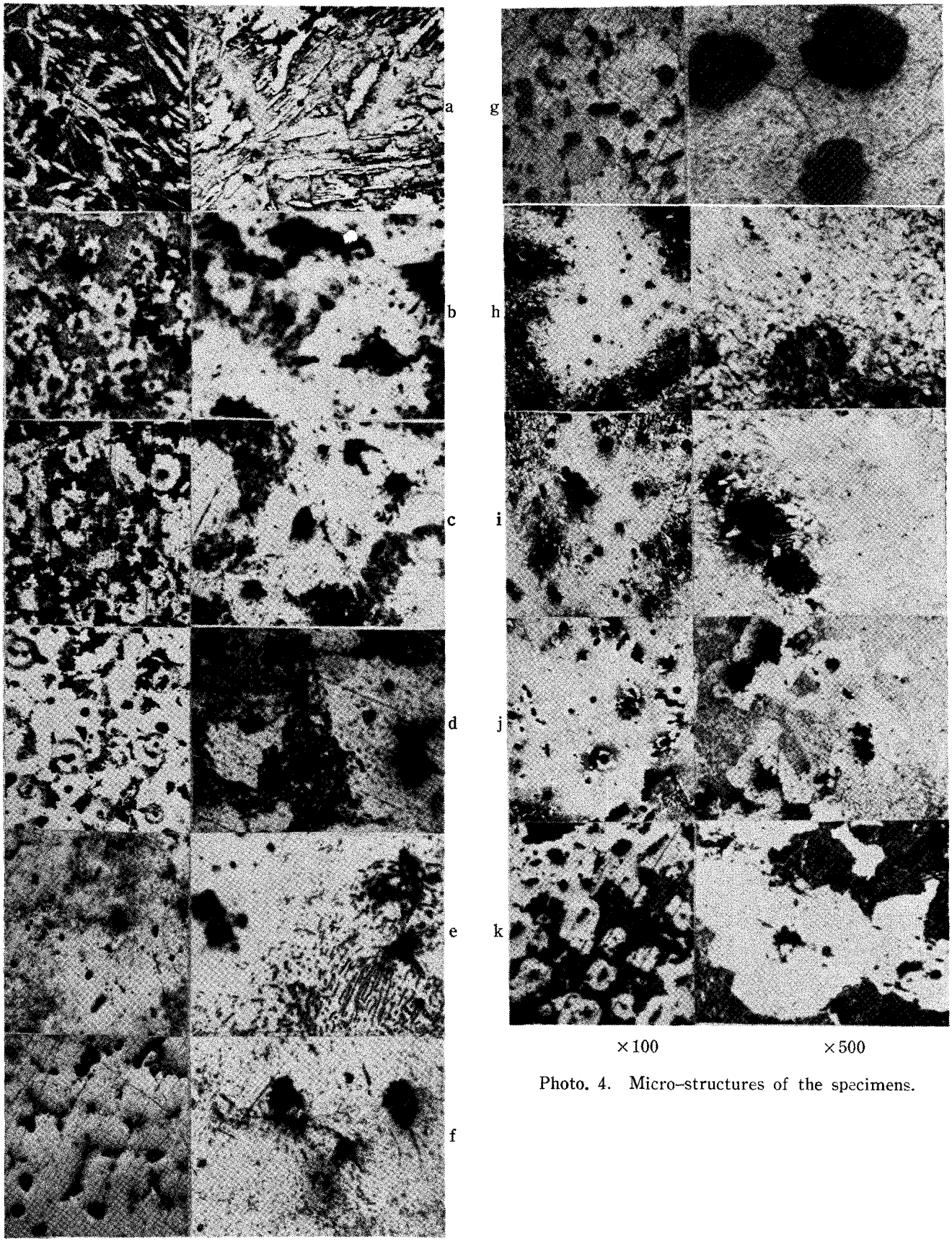

Photo. 4. Micro-structures of the specimens.

change in texture, similar specimen as a is heat-treated for very short durations successively. In h, eutectic cementite is left almost invariant, but in i and j cementite begins to decompose, graphite precipitates into fine spots and ferrite appears around it. With the progress in heat-treatment the structure of eutectoid cementite become thus decomposed and the hardness is lowered. In k, which is

Table 4. Conditions of casting of cast iron specimens.

Specimen	1	2	3	4	5	6	7	Spheroid graphite	Mottled
C %	3.6	3.6	3.6	3.6	3.6	3.6	3.4	2.8	3.6
Si %	2.2	2.2	2.2	2.2	1.8	1.8	2.2	2.8	2.2
Mold	Wet sand	Steel mold heated at 950°C	〃 600°C	〃 300°C	〃 800°C	〃 250°C	Sand	Sand	Steel mold
Size diameter	5 cm	6.5	6.5	6.5	6.5	6.5	5	5	4.5
Size length	25 cm	30	30	30	30	30	25	25	2.5
Graphite size (ASTM)	3	3–4	3–4	4–5	4–5	5	6	Mg treated	—

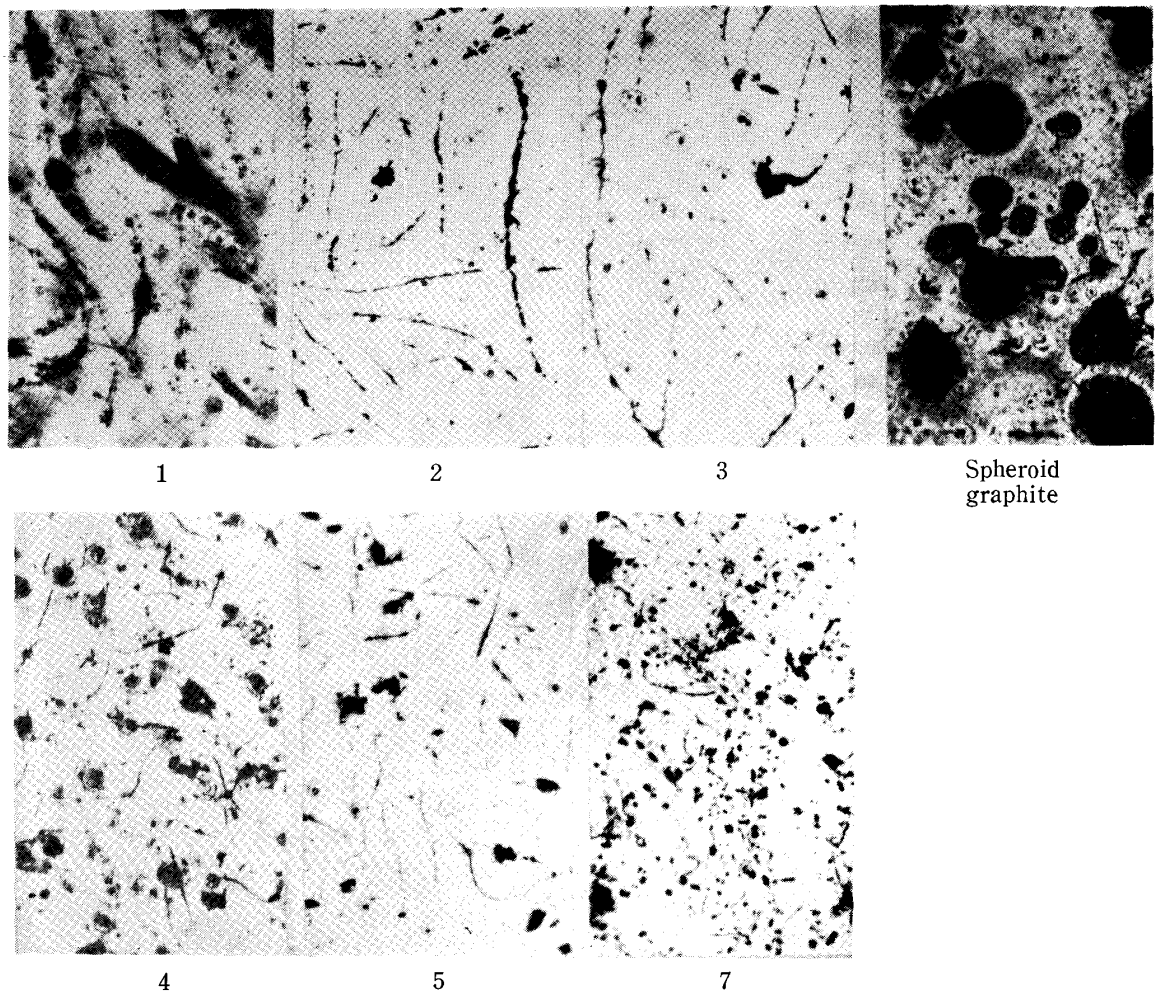

Photo. 5. Structure of the cast iron specimens. (×100)

kept at 900°C for an hour, the structure is quite similar to that in b and c, the bull's eye structure being apparent. In this case the total durations of keeping at 900°C are shorter, but the formation of graphite seems to have been rather accerelated.

3. Flake and spheroid graphite cast iron

The most useful materials are gray cast iron, and their structures are distributed in wide variation. Then the specimens of flake graphite cast iron and spheroid graphite cast iron were prepared and there were contained in these specimens the crystallized graphites of different shapes and sizes. The measurements of ultrasonic attenuation were carried out in these specimens and the correlations between the structures and the attenuation values were examined.

The specimens containing 3.4—3.6 per cent of carbon and 1.8—2.2 per cent of silicon were prepared by melting electrolytic iron containing 0.025 per cent of carbon with 99.99 per cent silicon and arc-carbon in a high-frequency electric furnace. To prepare the cast iron specimens of various structures, several types of mold were used and heating temperature and cooling rate of molds were controlled in wide range. The conditions of casting and the composition of the castings obtained are given in Table 4 and their structures were shown in Photo. 5. The resultant structure of the specimens were that of flake graphite cast iron in most cases, and mottled cast iron was obtained in steel mold of low temperatures. The sizes of the flake graphite in the gray cast iron specimens were within the range of No. 3–6 of the ASTM standards. The ingots were cut into cylinders of about 5 cm in diameter and in length respectively. To obtain the specimens of sound and homogeneous structure, the ingots were cut into several pieces and the flawless parts of idential structures at both end surfaces were selected. Then, a specimen of spheroid cast iron was made from the same melt by applying magnesium treatment. This ingot was heat-treated at 900°C for 2 hours and then for 3 hours and at last the structure of spheroid graphite and ferrite grains was obtained, the attenuation was measured at each stage.

As the cast iron is an alloy of several elements and has complicated structures, the factors influencing the ultrasonic attenuation are numerous and superposed each other. Thus, for determining the relations between the attenuation and the structure, it is most desirable to investigate the effect of a single factor, for example, only the size of the grains. But as the factors are almost unknown and difficult to divide into elementary one, the experimental procedure is limited in this study to take as invariant the common metallurgical factors, such as composition and general textures. In this procedure of preparation, the size of graphite is selected as a variable factor. However, so many specimens are used in this measurement and perhaps fine differences in the individual structure are left unknown, but, as detailed below, the measured results are found to vary in respect of the parameters expressing the factor under consideration without inconsistency. Then it will be concluded that important differences in the fine structure are removed from the specimens.

IV. The results of measurement

1. Steel

(i) Carbon steel and chromium-molybdenum steel

Examples of linear relation between the attenuation and the travelling distance of the ultrasonic waves are shown in Fig. 4. For the purpose of obtaining the attenuation coefficient, the exponential decay of ultrasonic waves (eq. (1)) was at first confirmed. The abscissa in the diagram is the distance travelled by the ultrasonic waves expressed in the number of their round trips through the specimen, and the ordinate is the attenuation values measured at the end-surface at every trip, the frequency being given alongside the curves. From the fact that this diagram contains only straight lines, it is deduced that the attenuation is of exponential type, and the slopes of these lines corresponding to the attenuation coefficients. From these values the attenuation coefficients can be obtained after correcting the loss of reflection at the end-surfaces.

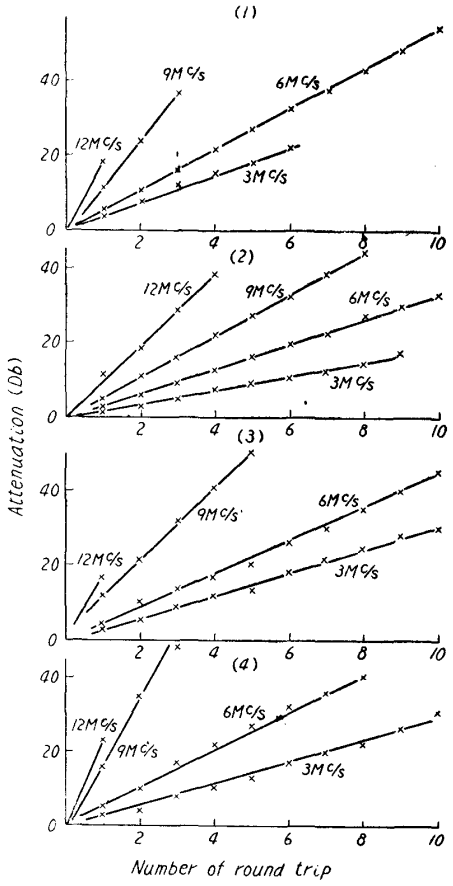

Fig. 4. Lineary proportional attenuation of ultrasonic waves as a function of number of round trips in specimens of (1) carbon steel k, (2) carbon steel i, (3) Cr-Mo steel k, (4) Cr-Mo steel l, respectively.

The curves a—m in Figs. 5 and 6 show such attenuation values per unit distance at each frequencies in the specimens subjected to different processes of heat-treatment. The form of the curves is markedly dissimilar for hardened and normalized specimens. The attenuation becomes larger as the frequency increases, so that it is usually impossible to make measurements at higher frequencies than 21 Mc/s.

The curve a illustrates the attenuation in forged specimens without heat-treatment. These specimens are of pearlite structure, in a′ lamellar pearlite is more abundant and in a″ spheroid pearlite is in predominance. Curve a′ shows a remarkably large attenuation and have a steeper slope than a″. In all these cases, attenuation measurement was possible at the frequencies lower than about 10 Mc/s. b is the results obtained with a hardened specimen of martensite structure. The attenuation value was fairly lower than in a and the measurement was possible up to 15 Mc/s. The curves c, d, e, f, g and h show the values on the specimen tempered at temperatures higher by 100°C for one hour successively. With the

progress of tempering the martensite structure of the specimen changed gradually into troostite and then into sorbite and the cementite precipitates became finer as shown in Photo. 1. The attenuation value decreased further with the progress

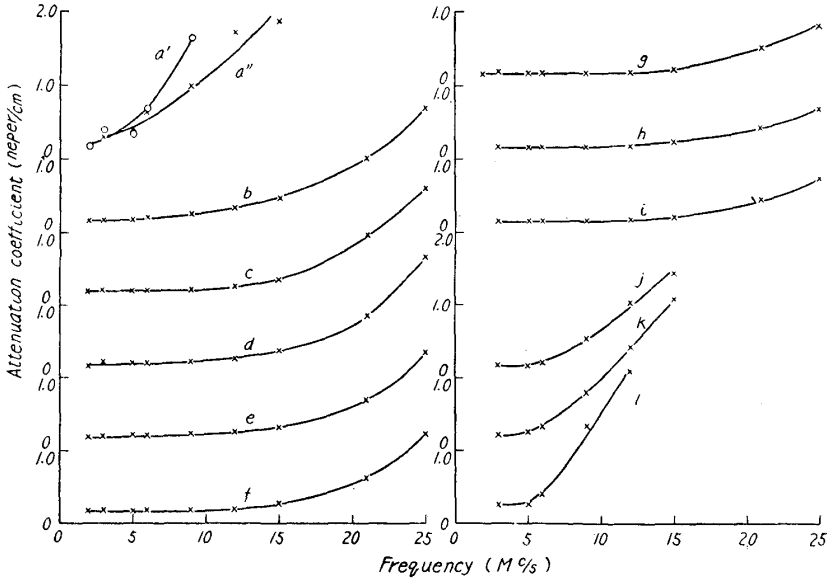

Fig. 5. Attenuation of ultrasonic waves in Cr-Mo steel under various heat-treatment. (See Table 1)

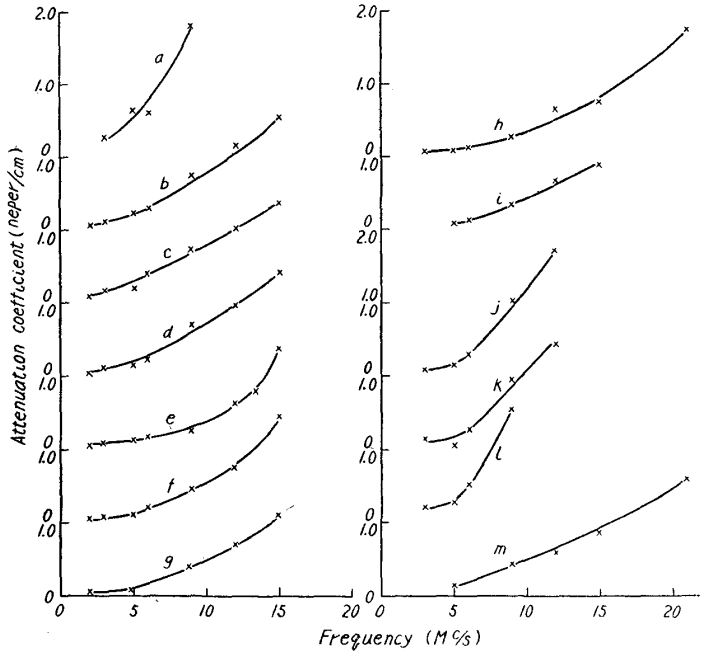

Fig. 6. Ultrasonic attenuation in carbon steel specimens at each stages of heat-treatment. (See Table 1)

of successive heat-treatment and the slopes of the curve became smaller. It will be concluded from this result that the finer structure in grains of steel results in diminishing of attenuation value. It is expected in the specimen tempered for long duration at just below the transformation point that the structure becomes

very fine and attenuation is very small. To confirm this the specimen was tempered for 5 hours at 680°C, and it was found that the slope was decreased as illustrated in i. Keeping the specimen for a longer time at this temperature, the attenuation will become still lower. Generally speaking, the attenuation increases linearly with frequency in lower frequency range and then rises steeply at higher frequency.

The Vickers hardness was measured at the end-surfaces of the specimen after each process of heat-treatment and the values are listed in Table 5. It is shown in this table that the hardness was increased by quenching and was reduced by

Table 5. Vickers hardness of the steel specimens.

Specimen		a	b	c	d	e	f	g	h	i	j	k	l	m
Vickers hardness	Cr–Mo steel	208	746	774	644	589	545	412	333	255	268	251	265	
	C–steel	216	696	669	610	539	493	397	319	244	258	274	270	600

repeated tempering and in the specimen annealed at 680°C for 5 hours, the hardness nearly returned to the initial value. But the hardness values do not give any clear indication of these attenuation characteristics directly, and close corelations between them cannot be confirmed.

The specimens of sorbite structure were then heat-treated at the temperatures higher than the transformation point, and the pearlite structures were formed again. The attenuation curves obtained in these pearlite structures were shown in Fig. 4 j, k and l. In comparison with the curves from b through i, the attenuation is found to be much intensified and the degree of intensification accompanying the rise in frequency also increases, so that it was impossible to make measurements at higher frequencies than 15 Mc/s. The values obtained here are similar to those obtained before hardening in a. The attenuation intensified further following each process of heat-treatment carried out at successively heightened temperature, and the increase of attenuation accompanying the increase of frequency also became steeper. These specimens had a pearlite structure, and the austenite grain size was as shown in Photo. 2. Proeutectoid ferrite is found at the grain boundaries of the original austenite. The uniform grain size distribution could not be attained and be classified into the ASTM number in the range of 7 to 9. The larger grain size was obtained with heat-treatment at higher temperatures. Since, however, the growth of grain was not so prominent, variation of the form of curves j, k and l in Figs. 5 and 6 is little. These data alone are not sufficient for determining the effect of the grain size on the attenuation, and this effect will be discussed thoroughly at the next section. The last curve m shows the attenuation in the specimen quenched into water from 1,000°C. The hardness was increased again as shown in Fig. 2 and the structure was of martensite. The attenuation values are small and the curve is similar in form with b.

All the measurements were carried out in similar way with either chromium-molybdenum steel or carbon steel. Considering from the structure as illustrated

in Photo. 1 and the attenuation values given in Figs. 5 and 6, the results obtained with these two kinds of specimens are in good agreement, and the changes following each process of heat-treatment are also similar in both specimens. From the results, it is concluded that the effect of heat-treatment is quite identical in the two kinds of specimens, so that the results initially anticipated have been arrived at. The ultrasonic attenuation in steel can be defined in correspondence with its microscopic structure, and the attenuation is reversible to the applied heat-treatment.

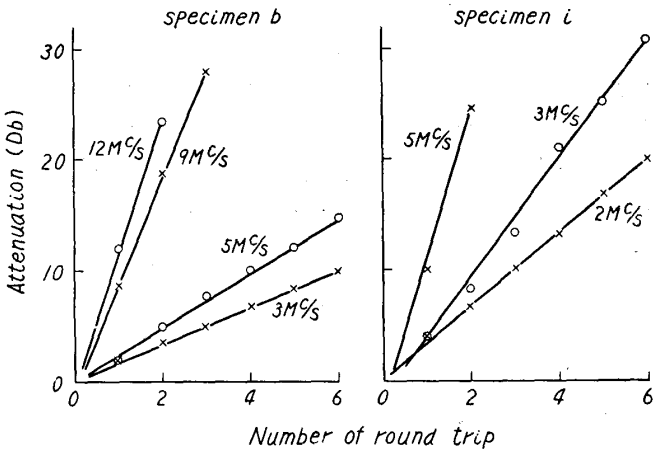

Fig. 7. Lineary proportional relations between ultrasonic attenuation and numbers of round trip in carbon steel.

(ii) The effects of grain size of carbon steel

The readings of the attenuator as plotted against the distance, that is, the number of the round trips through the specimens of carbon steel are shown in Fig. 7, in the unit of decibel. The specimens contain 0.75 per cent carbon, and have pearlite structures. The measured values are nearly on a straight line, and the attenuation under measurement is of the type as expressed by (1). The slope of the line varies with the ultrasonic frequency and also rather drastically with the heat-treatment of the specimen, that is to say, the grain size of the specimen.

As the slopes of the straight lines in Fig. 7 represent α in (1), the attenuation values are directly obtained from the figure. The change of attenuation coefficients with the frequency are illustrated in Fig. 8. To save the space the lines indicating the attenuation coefficient zero and ditto 0.1 are drawn in coincidence in the same figure. The

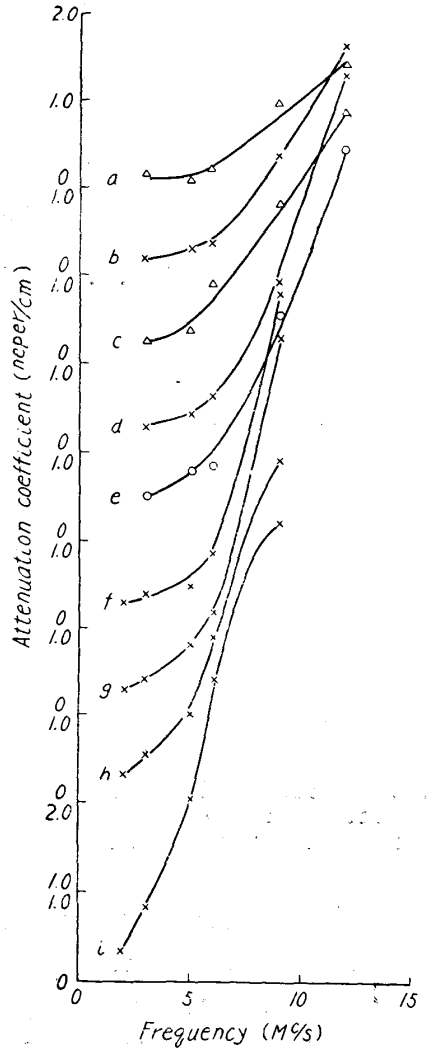

Fig. 8. Ultrasonic attenuation in normalized carbon-steel with various grain sizes.

letters a, b, c and so forth indicate the last process of heat-treatment corresponding to those in the first column of Table 2, with the progress of heat-treatment grain size of the specimen becomes larger.

As seen from the curves in this figure, when the grain size is fine the attenuation has a constant value and unaffected by a change in frequency at the lower frequencies, but abruptly rises in value when the frequency approaches 10 Mc/s. As the grain size becomes larger, the range of constant attenuation at low frequency side diminish and the frequency at which the attenuation suddenly begins to rise becomes lower. Then, the attenuation at higher frequencies becomes very large and the values can be obtained. The first curve a and the last curve i are so radically different in form.

The values of attenuation given in the above figures have been measured by the pulsed pattern of ultrasonic waves appeared on the oscilloscope. When a reflection pattern as shown in Photo. 6 appears on the oscilloscope, the readings

Photo. 6. Oscillogram of pulsed ultrasound in the specimen b at 5Mc/sec.

of the attenuator are shown in Fig. 7, and the ultrasonic energies are dissipated with the exponent of the path length. When the grain size has grown owing to successive processes of heat-treatment, a reflection pattern as shown in Fig. 9 was obtained at high frequencies. If only the first 2 or 3 pulses are taken into account the attenuation value might be calculated, but the later pulses are not usable, because of the irregularity of their height and sites, and the exponential type attenuation can not be obtained. For example, in specimen i, the value at 9 Mc/s and the value obtained from the earlier three pulses at 12 Mc/s are equal. But, some of the later pulses at 12 Mc/s, are not remarkably different in height from the earlier, showing a large deviation from the exponential type, then the data are omitted. Such disturbances in the pulse patterns are thought to be due to the diffuse transmission of the ultrasonic waves through the specimen deviating gradually from the initial direction of travelling, and the resultant pulses are received as the sum of each

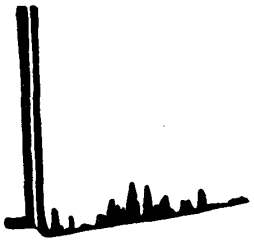

Fig. 9. Schematic oscillogram of anomalous patterns obtained in specimen g at 12 Mc/s.

diffused component with same total path length disregarding the individual path. As the specimens consist of elementary grains of slightly varying elasticity in the direction of sound transmission, this will be discussed in detail at the last section, the beams of ultrasonic waves are reflected and refracted at the boundaries of such grains and the diffused beams are then reflected at the side surfaces of the specimens. Such irregularities cause the random paths of the waves varying widely in length, and moreover there may occur a transformation from longitudinal to shear waves and vice versa at any reflection or refraction. At last the series of ultrasonic pulses, when finally received, show irregularly mixed phases and amplitudes, causing mutual interference and resulting in such deformed patterns of the pulses.

2. Cast iron

(i) White cast iron

Ultrasonic attenuation in cast iron has some identical features with those of steel, but special characteristics are also observed, the details will be given in this section. Fig. 10 shows the values of attenuation coefficient versus number

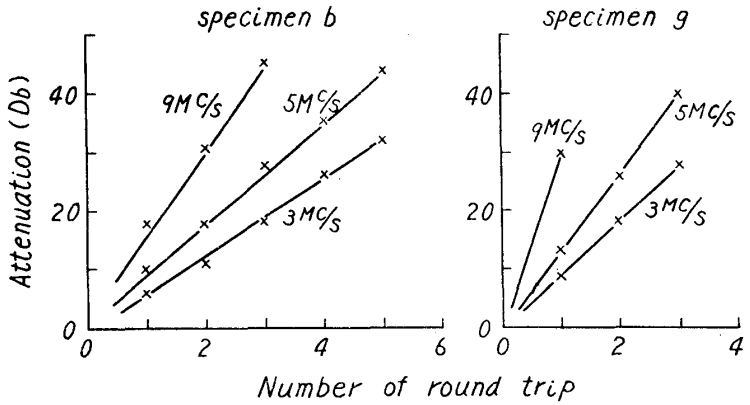

Fig. 10. Linear relations between logarithmic attenuation and numbers of round trip in cast iron specimens.

of round trip of pulses in white cast iron and of spheroid graphite cast iron specimens obtained by annealing the former. As the figure shows, the attenuation increases linearly with the path length and the rate of increase correspond to α in the equation (1), values of α being found to be considerably varied according to the frequency. The reflection loss of the ultrasonic waves at the end-surfaces of the specimen is included in measured values of α here. In the measurement on the steel specimens, such a loss was found to be about 1.5 db per reflection, and this loss in cast iron is presumed to be of the same order. But since the measurement of the loss was not carried out owing to limitations in specimens, the data given in this section were not corrected for the loss.

As the structure was changed by heat-treating the specimens of white cast iron, the ultrasonic attenuation was changed gradually as illustrated in Fig. 11, measured with each specimen as shown in Fig. 10.

The patterns appearing on the oscilloscope are as shown for example in Photo. 7. As the frequency was raised, the pulses appearing at the oscilloscope became lower in their height and at last no pulses were observed at about 15 Mc/s. And in some cases, irregular pulse patterns were observed and the attenuation coefficient could not be measured.

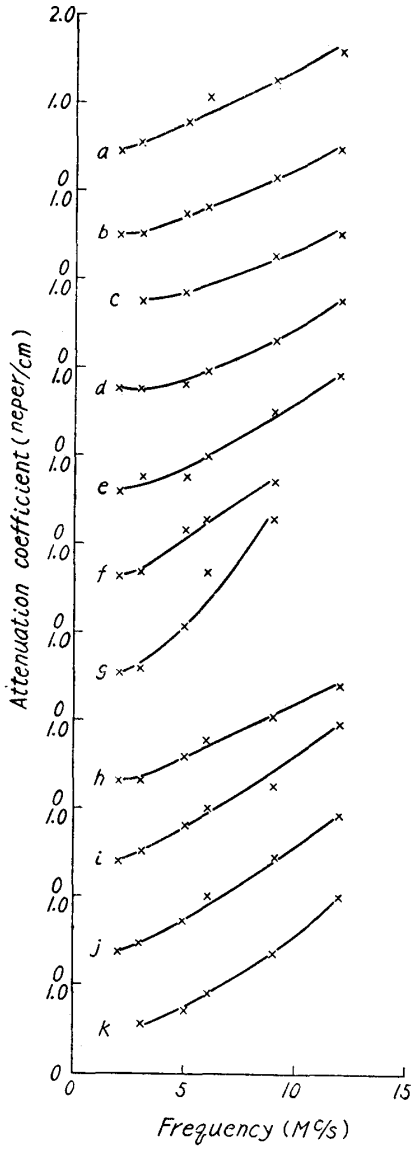

Fig. 11. Attenuation coefficient in white cast iron specimen.

In Fig. 11, there are remarkable differences between the curves a and g in their form. The attenuation of low frequency waves becomes smaller in g than in the earlier stages of annealing, but that of high frequency waves on the contrary becomes much larger in the later stages of annealing, finally increasing beyond measurement. In the intermediate stages of annealing, the change in attenuation is gradual. In a and b, the attenuation value is smaller in b at medium frequency, while in c, the value at low frequency is higher than in b, though the curves are similar in form in the two. With the advance of annealing in d and e, the attenuation value increases at high frequency, however, regard to structure, the differences between the specimens from b to e are little, only a few variation of concentration of graphite, pearlite and ferrite are observed. Thus, the difference in form of the attenuation curves corresponds to the exhaustion of pearlite and the increase of ferrite and graphite. At the beginning of graphitization, before graphite comes forth in distinct existence, there occurs some alteration in attenuation. In i through k, we find that the attenuation is intensified at high frequency in i and f, and that the value in k is uniformly lower than in a.

(ii) Flake and spheroid graphite cast iron

The ultrasonic attenuation coefficients in flake and spheroid graphite cast iron specimens are summarized in Table 6 and Fig. 12 with respect to ultrasonic frequency. In any of the specimens the attenuation coefficient was small at 0.5 Mc/s, but with the rise of the frequency, the attenuation increased steeply and it became impossible to measure at the frequencies of several megacycles per second. The pulse patterns appearing on the oscilloscope were of the type shown in Photo. 8, and the regular transmission of ultrasound was verified at low frequency. But when the frequency became higher, the figure became irregular. Such irregular

patterns are similar in type with those obtained in various metals and alloys and these patterns are frequently found to appear in the range where the wave-length of the ultrasonic waves is smaller than the size of grains. In the present specimens, these grains are surrounded by flake graphite, and what is most notable

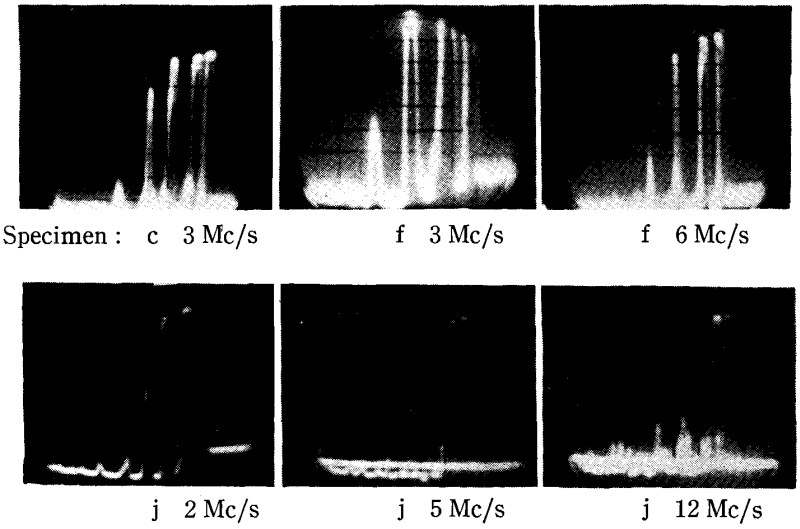

Photo 7. Oscillograms of ultrasound.

Table 6. Ultrasonic attenuation coefficient in flake and spheroid graphite cast iron. (db/cm)

Specimen / Frequency	1	2	3	4	5	6	7	Mottled	Spheroid graphite 900°C 2 hour
0.5 Mc/s	0.3 db/cm	0.24	0.2	0.2	0.3	0.35	0.16	0.13	0.22
1	—	1.2	1.1	0.6	0.45	0.37	0.35	0.3	0.32
2	—	—	—	—	—	1.3	—	0.4	0.47
3	—	—	—	—	—	—	1.5	0.63	0.64
5	—	—	—	—	—	—	—	—	0.81

here is that there is a close relation between the size of the flake graphite grains and the value of ultrasonic attenuation. For example, with a specimen containing flake graphite of size number 3, the attenuation measurement could not be carried out at 1 Mc/s, while with a specimen with graphite of number 6, it was possible to measure the attenuation at 3 Mc/s. The highest frequency at which the reliable measurement was feasible rose as the grain size of graphite was reduced. The flake graphite cast iron specimens are composed of flake graphite and pearlite grains, and the results obtained in these measurements may be applied to all kinds of gray cast iron, disregarding

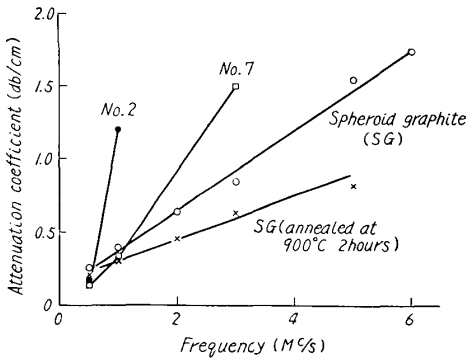

Fig. 12. Attenuation of ultrasonic waves in flake, spheroid graphite cast iron and annealed specimens.

the small differences in the laminated structure of the pearlite matrix.

In comparison with these flake graphite cast iron, the attenuation coefficients in spheroid graphite cast iron are lower and the measurements are carried out even at higher frequencies. In fact, the attenuation values are similar to that in malleable cast iron prepared from white cast iron by annealing. Regular figures of pulse patterns are observed as illustrated in Photo. 8. When the matrix is

i) gray iron 0.5 Mc/s 2 Mc/s 3 Mc/s

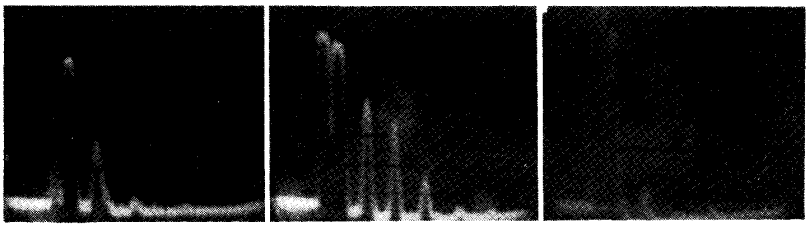

ii) SG iron 1 Mc/s 2 Mc/s 3 Mc/s

Photo. 8. Oscillograms of ultrasonic wave i) in gray cast iron No. 1, and ii) in spheroid graphite cast iron.

exhausted in cementite and changed into ferrite, the attenuation values are remarkably reduced, just as in malleable cast iron. It is found that even when the content of free graphite is the same, the attenuation of ultrasonic waves is higher in the specimen containing flake graphite than those with spheroid graphite. Mottled cast iron has an intermediate features between white and gray cast iron in structure, and in the specimen prepared now, the graphite is found mostly in the form of small flake and formation of eutectic cementite is little. So the attenuation is not much different from that in gray cast iron in general and irregular pulse patterns begin to be observed at 5 or 6 Mc/s.

V. Discussions on the results

1. Steel

(i) The effects of structure in chromium-molybdenum and carbon steel

There are many factors influencing the ultrasonic attenuation in solids in the megacycle frequency range, and almost all of these have been unsolved owing mainly to their complicated features. In polycrystalline metals and alloys of single phase region, the ultrasonic attenuation changes with their grain sizes. And in these metals, such as aluminum, the various results of investigations on the relations between ultrasonic attenuation and frequency have been published and clear interpretations have been given. According to the results of these measurements,

the ultrasonic attenuation rises steeply with frequency at wave-lengths approximately equal to the size of the crystal grains. And the amount of this attenuation increases in proportion to the second to fourth power of the frequency. According to Rayleigh's analysis the scattering of elastic waves is caused in the medium by a *domain* of slightly different elasticity when the wave-length is comparable with the size of the domain. And the energy loss by the scattering is proportional to the difference in elasticity between the medium and scatterer and to the fourth power of the frequency. Since such an attenuation was observed in specimens of various grain sizes, it may be concluded that the scattering by domains with different elasticity and of comparable size with wave-length in the medium, that is, the elementary crystal grains, plays the leading part in the ultrasonic attenuation.

In discussing the origins of ultrasonic attenuation in steel, it is necessary to point out that the textures are very complicated and are altered to a large extent by heat-treatment. For example, lameller pearlite appears in normalized steel and martensite structure in hardened one, then the difference in the feature of ultrasonic attenuation in these steels must be considered from the difference in the texture. Then, at first, the effects of austenite grains on the ultrasonic attenuation will be discussed in normalized steel, and then the considerations on the effects of structure differences among pearlite, martensite and its annealed structures will be given.

As shown in Photo. 2, the average diameters of austenite grains were distributed between 0.02 and 0.03 mm, while the wave-lengths of ultrasonic waves were in the range between 0.2 and 10 mm approximately. Then the latter is several folds to some scorefolds as large as the diameters of the former. In aluminum polycrystals in the former case, grain diameters are in similar relations with wave-lengths as in the present case, and the scattering by the elementary grains is considered to be a cause of ultrasonic attenuation in steel as well as in aluminum. In the measurement in wide range of frequency the ultrasonic attenuation becomes large at the region where the wave-length is similar in size with grain diameter. If Rayleigh's law of scattering is applicable, the scattering of waves with wave-length longer than the grain increases with the fourth power of the frequency. In the hypoeutectoid structure shown in Photo. 2, ferrite layer is segregated at the boundaries of the original austenite grains, and the main parts of grains are composed of pearlite structures, hence it is considered that these grains form the scattering centers of ultrasound. The steep rise of attenuation accompanying the rise in frequency as in Fig. 4 a, j, k and l may correspond to the energy loss of ultrasonic waves in proportion with the fourth power of frequency; the precise analysis of the effects of grain size will be given in the next section. In the former report, it was pointed out that the impurities segregated at the grain boundaries are a cause of the higher attenuation in impure aluminum than in pure aluminum. Just in the same manner, the thick layer of ferrite boundary reflects the ultrasonic waves and increases the attenua-

tion. The pulse pattern of ultrasonic waves of 21 Mc/s in a pearlite specimen is shown in Fig. 13. The directly received pulse lies at the left end, next is the pulse received after a trip of one round, and in the following interval, random pulses are appeared. These irregularities must be due to the random propagation of the ultrasonic beams through the specimen suffering from the irregular reflection and refraction at the grain boundaries. Such an irregular pattern was observed only when the high frequency ultrasound was used. In such a case the observable regular reflection pulses are reduced in number, then the measurement of attenuation becomes impracticable.

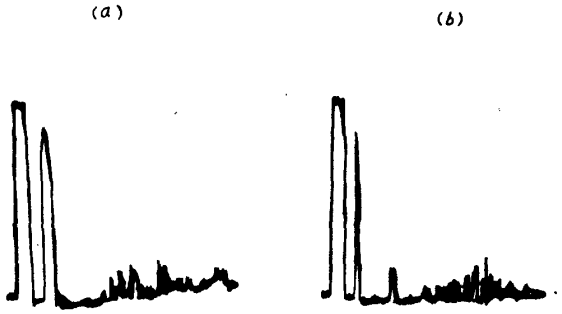

Fig. 13. Anomalous patterns of ultrasonic pulses.
(a) in Cr-Mo steel j at 21 Mc/s and
(b) in carbon steel k at 15 Mc/s.

On the other hand, the homogeneous structures of martensite are formed by hardening so that such abnormal reflection patterns are not observed and the attenuation values are much smaller than in pearlite. When such a hardened structure is tempered, the precipitated cementite particles become fine and the original austenite grains become isotropic and have less effect for ultrasonic propagation than pearlite. In this case, the grain size is quite smaller than the wave-length of the ultrasonic waves, so that in the range of low frequency the attenuation coefficient is almost constant and nearly independent of frequency. The scattering of sound waves becomes perceptible only in the frequency range where the wave-length is about tenfold of the grain size owing to the small anisotropy of grains. This consideration will be permitted regarding with the attenuation features as shown in Figs. 5 and 6 where the attenuation coefficient steeply rises at the frequency of about 15 Mc/s.

In summary of these considerations, it will be concluded that the ultrasonic attenuation in steel is mainly due to the Rayleigh scattering of ultrasonud by austenite grains. And the remarkable differences of ultrasonic attenuation between pearlite and martensite structure are originated mainly from the difference in the degree of elastic anisotropy of austenite grains, whether they contain lameller pearlite or small particle of cementite. The martensite and its annealed structure will be less anisotropic than pearlite structure, and the ultrasonic attenuation in the former is small even at high frequencies as 20 Mc/sec.

(ii) The effect of grain size in carbon steel

Now, we will consider the ultrasonic attenuation in steel of pearlite structure in detail with respect to grain size. The specimens are composed of pearlite grains surrounded by proeutectoid ferrite boundary, only the grain size being different in different specimens. In the previous report on aluminum, it is concluded that the scattering of ultrasonic waves by crystal grains is the predominant origin of

attenuation, and the attenuation coefficient is well represented by the fourth power relations with frequency. In the range where the ultrasonic wave-length is larger than the grain size, the attenuation coefficient α is expressed with frequency f by the relation

$$\alpha = B_1 f + B_2 f^4 = \alpha_1 + \alpha_2, \qquad (3)$$

where $\alpha_2 = B_2 f^4$ is the attenuation resulting from the scattering of sound waves by crystal grains. According to Rayleigh's scattering formula of sound B_2 is represented as

$$B_2 \propto K \cdot V, \qquad (4)$$

where K is the space average value of the square of the elastic anisotropy of elementary grains[3], and V is the averaged volume of the grains. $\alpha_1 = B_1 f$ corresponds to the loss due to elastic hysteresis in the range of low frequency, and the loss of energy per cycle is frequency independent and proportional with coefficient B_1. There are no reliable analysis that B_1 is exactly constant in the higher range of frequency. But in this case, in such a range α_2 becomes larger in value, and the contribution of α_1 to the attenuation will becomes negligible. When the measured values in Fig. 6 are expressed by the formula (3), the coefficients B_1 and B_2 take the values as listed in Table 7.

Table 7.

Specimen	a	b	c	d	e	f	g	h	i
B_1 $\frac{\text{neper}}{\text{cm}}$ $\frac{1}{\text{Mc/s}}$	0.066	0.063	0.13	0.084	0.11	0.067	0.11	0.12	0.21
B_2 $\frac{\text{neper}}{\text{cm}}$ $\frac{1}{(\text{Mc/s})^4}$	0.301×10^{-4}	0.85	0.69	1.59	2.26	3.65	5.26	8.4	16.3
Grain size number	7–8	6–7	6–7	5–7	5–7	5–6	4–6	4–5	3–4

In this table the value of B_1 is almost unaltered for the change in the grain size of austenite; it may be concluded that B_1 has a constant value and this will confirm that the hysteresis constant B_1 is independent of the grain size.

The value of B_2 varies widely according to the difference in grain size. In this case, the austenite grains are assumed to be the center of scattering, as the grains are not much different in size from the wave-length of the ultrasonic waves. But there are remarkable differences between the grains of aluminum and steel, the latter including more complicated structures than the former. The attenuation values in the steel specimens are much larger than in aluminum, and differ remarkably corresponding to the fact that the structure of specimen is pearlite or martensite, even if their grain sizes coincide each other.

According to the relation (4), B_2 is proportional with the term representing the elastic anisotropy and the volume of the grains. Now the ratio between B_2 and the volume of grain have values as shown in Table 8. Regarding this

table it is found that this ratio has a mearly constant value, approximately 2×10^3, and from this the value of K in (4) is calculated as about 4.2. This value may be taken to express the elastic anisotropy of pearlite grain. In light alloys, this

Table 8.

Specimen	a	b	c	d	e	f	g	h	i
Volume cm^3	0.15×10^{-7}	0.35	0.48	0.7	1.2	1.6	2.5	4.0	9.3
B_2/Volume $\frac{\text{neper}}{cm^4}\frac{1}{(Mc/s)^4}$	2×10^3	2.4	1.5	2.3	1.9	2.3	2.1	2.1	1.8

value is about 10^{-3} times of the above according to the measurements of Mason and others in 17ST, and in pure aluminum it is even smaller. Now it may not be easy to infer that the anisotropy of pearlite structure is thousand fold as large as that of aluminum, but some acceptable conclusions can be obtained: The elastic anisotropy of α-iron of body centered cubic crystal as calculated in polycrystals is about 30 folds of that of aluminum. In lamellar pearlite structure, the elastic properties of the alternated layers of α-iron and cementite must differ fairly and there are wide differences between the elastic properties of the pearlite grain in the direction parallel and vertical to the lamination. Thus the value of anisotropy in pearlite structure is probably much larger than that in α-iron, and the multiplier 10^3 cited above is considered as a fairly meaningful. The difference between the attenuation values of pearlite and martensite is attributed to the larger elastic anisotropy of pearlite, since there is no difference in grain size.

From such considerations, the interpretation that the ultrasonic attenuation in pearlite steel is due to the scattering of the waves by the original austenite crystal grains may be deemed as justified.

2. Cast iron

(i) White cast iron

There are remarkable differences between the ultrasonic attenuation in white cast iron and in spheroid graphite cast iron. Considering from the above measurements, it is found that the fine structure in the texture of cast iron is the origin of these attenuation characteristics, and the attenuation is determined by elastic anisotropy in elementary structures. In the case of specimen h prepared by annealing the specimen a for 15 minutes, crystallized cementites were dispersed in pearlite matrix, and their graphitization was scarcely observed. Then the elements of the structure are very fine and distributed uniformly to reduce the elastic anisotropy and the attenuation is reduced. In i and j, the graphitization advances with the degree of annealing resulting in the coarse grain structure and the attenuation due to the scattering of sound waves occurs in high frequency range, showing figure rather resembling that of a. In the specimens b, c and k, where the bull's-eye structure of ferrite make appearance, the areas of pearlite and ferrite region become large in the matrix at the expense of cementite zone, the

attenuation is increased even in the low frequency range. It will be estimated that the amount of elastically anisotropic pearlite domain will have large effects on ultrasonic attenuation. In the specimens d and e, the area of pearlite domain is reduced and ferrite domain is enlarged, so that the low attenuation values in the low frequency range were observed. But the graphite grains simultaneously grow considerably in size, and these grains have an elasticity very widely different from that of ferrite, then the attenuation rises in the high frequency range. In g, where the graphitization is nearly accomplished, the attenuation is drastically reduced to a value, which may probably approximate that of attenuation in α-iron composed of ferrite grains. In the higher frequency range, the ultrasonic waves are scattered by ferrite and also by graphite grains, so that the attenuation values increase to considerable extent. But, generally speaking, in white cast iron and in black-cored malleable cast iron prepared by tempering the former, the attenuation coefficient of ultrasonic waves is fairly low in the frequencies up to several megacycles per second. Then there will be no inconviniences in carrying out the flaw detection of these materials.

(ii) Flake graphite and spheroid graphite cast iron

Flake graphite and spheroid graphite cast irons consist of ferrite, pearlite and graphite in structure but the shape of graphite is very complicated, varying from flake to spheroid. Considering the structure of these cast irons, their microstructures are similar with that of steel, and the results obtained with the measurements of ultrasonic attenuation in steel will be applied to that of cast iron. The ultrasonic attenuation in cast iron has remarkably larger values than in normalized carbon steel, but the general features of attenuation that the values steeply rise with a rise in frequency shows a close similarity with those obtained in steel. In steel specimens, it is ascertained that the ultrasonic waves are scattered by austenite grains having grain size comparative with wave-length and lose the energy. In this case the main factor determining the amount of the scattered energy is the large elastic anisotropy of pearlite grains, and the same circumstances are also in the case of cast iron. The specimens of flake graphite cast iron are composed of pearlite structure, and the shell-like graphites are distributed therein in the same manner as the ferrite grain boundaries in proeutectoid steel.

If such grains of pearlite structure cause scattering of ultrasonic waves commensurate in wave-length to the grain size, there will be a relation between the frequency and the attenuation coefficient α as illustrated in the formula (3). Applying this formula to the measured values the coefficients B_1 and B_2 would be calculated, and the values are listed in Table 9. Here, B_1 has an approximately constant value of about 0.4 db/(cm-Mc/s) while B_2 varies in a considerable range. B_2 is a quantity changing in proportion to the elastic anisotropy and the volume of the grains of pearlite structure, as in the relation (4). Then the ratio of B_2 to the volume of grain, represented by the volume surrounded by the flake graphite, has a definite constant value, 3×10^4 db/(cm-Mc/s)^4 as shown in the last row of Table 9. The value of this ratio corresponds to the degree of elastic anisotropy

of pearlite grain and this is a quantity to be compared with the elastic anisotropy obtained in other metal crystals. For example the measured value in 17ST has been reported as 2.7 db/(cm-Mc)^4 and in carbon steel, as 2×10^4 db/(cm-Mc/s)^4.

Table 9.

Specimen	2	3	4	6	7
Grain size number	3–4	3–4	4	5	6
B_1 $\frac{\text{db}}{\text{cm}}$ $\frac{1}{\text{Mc/s}}$	0.38	0.3	0.37	0.42	0.46
B_2 $\frac{\text{db}}{\text{cm}}$ $\frac{1}{(\text{Mc/s})^4}$	0.82	0.8	0.23	0.031	0.003
Volume cm^3	27×10^{-6}	27	8	1	0.1
B_2/Volume $\frac{\text{db}}{\text{cm}^4}$ $\frac{1}{(\text{Mc/s})^4}$	3×10^4	3	3	3	3

The value now under study is of the same order as that of carbon steel, but is too large in comparison with those of ordinary metals. But the value is in good agreement with those in steel, calculated similarly under the assumption that the pearlite grains are the center of scattering. As the pearlite structure is composed of alternating thin layers of cementite and ferrite, the difference of elasticity in different directions will be large. From this fair coincidence of the value in these two cases, it will be concluded that ultrasonic attenuation in normalized steel and flake graphite cast iron is originated from the scattering of sound waves by the elastically anisotropic pearlite grains.

The elasticity of graphite grains differs from that of iron, and the difference in the acoustic properties will be large between them, then the effect of graphites on ultrasonic attenuation is a next problem. The ultrasonic pulse patterns in flake graphite cast iron are shown in Photo. 8; at high frequency the irregular pattern is observed as in pearlite carbon steel. This is interpreted as due to the diversity of the path of ultrasonic waves caused by reflection at the thick ferrite layers formed at the original austenite grain boundaries. In the flake graphite cast iron, the shell-like graphite crystallites take the place of grain boundaries of the pearlite. And since their elasticity is very different from that of the matrix phase, then the confused pattern is due to a similar cause.

In spheroid graphite cast iron, the graphite crystallites take the spheroidal form and with annealing the increase of ferrite in expense of pearlite is observed. With the advance of annealing process the matrix becomes a polycrystal structure of ferrite grains with graphite crystallites of a similar size dispersed in them, and the attenuation value becomes much smaller than in untreated specimen. The lower attenuation in spheroid graphite cast iron than in flake graphite cast iron in high frepuency range is attributable to the diminution of pearlite matrix. Since the elastic anisotropy of pure ferrite grains is far smaller than that of pearlite grains, the attenuation due to scattering in spheroid graphite cast iron

is suppressed to a large extent.

Based upon these considerations, practical procedures for the ultrasonic testing of cast iron will be considered here precisely. In flake graphite cast iron, the lower frequency waves between 0.5—2 Mc/s may be used with advantage, the larger the graphite grains the longer wave-lengths being required. With spheroid graphite cast iron including spheroidal graphite grains, it has an advantage of accurate results to make use of ultrasonic waves of 3—6 Mc/s. In cast iron containing fine graphite grains or eutectic cementite, ultrasonic waves of 1—6 Mc/s may be used, and the most favorable conditions can be selected regarding with the testing materials.

As a result of this measurement some informations are obtained for the nature of the ultrasonic attenuation in steel and cast iron, and the origin of attenuation in such materials. The attenuation of ultrasonic waves is closely dependent on the structure of the materials, a change in structure producing a remarkable difference in the features of attenuation. The structures of steel and cast iron are composed of some elastically anisotropic domains, and their size is comparable with the wave-length of ultrasonic waves of the megacycle frequency range. For example, in steel of pearlite structure, the grain size of pearlite is distributed from 10^{-1} to 10^{-3} mm. These grains scatter the ultrasonic waves, resulting in diminution of the energy of received waves and this is the main cause of ultrasonic attenuation. The large difference of elasticity by different directions of the pearlite structure in granular graphite cast iron is the cause of the high attenuation of sound waves. This elastic property of pearlite grain has the same effect on ultrasonic attenuation in steel and cast iron. It is also successfully explained how the ultrasonic attenuation varies widely with the structure of steel prepared by heat-treatment such as hardening and tempering, and how ultrasonic waves attenuate in as cast structure and in structures of heat-treated cast iron. Considering from these data, the most favourable method of ultrasonic flaw detection of steel and cast iron may be designated. Then the standard procedures of testing, as well as the accuracy of such procedures may be precisely determined.

In conclusion the author wishes to express his sincere thanks to Professor Tokutaro Hirone of the laboratory for his guidance throughout this work and to Professor Yosimitu Kikuti of the Research Institute of Electric Communication, Tohoku University, and Mr. Rokuro Utida of Japan Radio Co. Ltd. for their valuable suggestions in the method and apparatus of measurements. And his hearty thanks are also due to Professors Yûnoshin Imai and Masao Homma of the Research Institute for Iron, Steel and Other Metals, Tohoku Univsersity and also to members of their laboratories for their kind suggestions in preparing the specimens.